List of Changes

April 1, 2025

All sections, paragraphs, and figures refer to the revised manuscript. In the marked-up version of the revised manuscript, all changes are highlighted in red.

1) **We added a version number to the title.**

   ICON-HAM-lite 1.0: ...

2) **In the abstract, we revised the first sentence.**

   ... nuclei for cloud droplets and ice crystals.

3) **In the abstract, we revised the last sentence.**

   ... the emission of dust aerosols by cold pool outflows in the Sahara and the interaction of sea salt aerosols and shallow convective storms around the doldrums.

4) **In section 1, we revised two sentences in the second paragraph.**

   ... decades (Tegen et al., 2019). ... few years.

5) **In section 2.1, we revised a sentence in the first paragraph.**

   ..., also referred to as dry radius, ...

6) **In section 2.1, we revised a sentence in the second paragraph.**

   ... dry radius ...

7) **In section 2.1, we added a sentence to the second paragraph.**

   The wet radius and density are used throughout the calculation of aerosol processes as described in section 2.3.

8) In section 2.1, we added three sentences to the last paragraph.

We acknowledge that the one-moment scheme HAM-lite has limitations in comparison to the two-moment scheme HAM. Since it carries no information about the aerosol size, there is no explicit representation of nucleation, growth, and ageing. And there is no ability to adjust the aerosol size in response to activation and wet deposition (Stier et al., 2005; Siebesma et al., 2020).

9) In section 2.2, we corrected a sentence in the second paragraph.

There are three parameterization schemes, one for cloud microphysics, one for radiation, and one for turbulence ...

10) In section 2.2, we added revised a sentence in the second paragraph.

The cloud droplet number and ice particle number are not prognostic but prescribed or diagnosed.

11) In section 2.2, we added a paragraph.

Partially resolved processes such as shallow convection or orographic drag are not parameterized. As outlined by Hohenegger et al. (2023), there are three main reasons for this choice. First, a lean code with few parameterization schemes can be ported more easily to new systems such as the new exascale cluster of the Forschungszentrum Jülich (2025). Second, parameterization schemes do not converge as the resolution is refined, which would be problematic for future simulations with ever increasing resolutions. Hohenegger et al. (2020) showed that some large-scale quantities such as net shortwave radiation start to converge at resolutions of about five kilometers. Third, ICON-MPIM is intended for Earth system research and not operational weather forecasting. Simple physics make it easier to understand, for example, the impact of processes that remain partially resolved or parameterized at kilometer scales.

12) In section 2.3.1, we added two sentences to the first paragraph.

Due to the absence of microphysical processes, emissions are directly added to modes without any intermediate steps. In reality, precursor gases such as sulphur dioxide form secondary aerosols by nucleation (Siebesma et al., 2020).

13) In section 2.3.1, we replaced the reference to Tegen et al. (2019) with Tegen et al. (2002) in the first paragraph.

... Tegen et al. (2002), ...

14) In section 2.3.1, we revised a sentence in the first paragraph.

The mass fluxes from the emission sectors are converted into number fluxes based on the radius of average mass of the mode, i.e.,

$$F_{\mathrm{em},j,k,s} = \frac{3}{4\pi \bar{r}_{\mathrm{m},j}^3 \rho_k} S_{\mathrm{em},k,s}, \tag{1}$$

where $S_{\mathrm{em},k,s}$ is the mass flux of species k in sector s.

15) In section 2.3.6, we corrected the spelling of asymmetry.

... asymmetry ...

16) In section 3.1, we revised the caption of table 2.

Dry radii ... Standard deviations (σ) of modes were also taken from ECHAM6.3-HAM2.3, i.e., 2.00 for the dust and sea salt modes and 1.59 for the carbonaceous and sulfuric modes.

17) In section 3.1, we added the three sentences to the second paragraph.

The biogenic emissions were taken from Guenther et al. (1995). As in HAM (Stier et al., 2005; Tegen et al., 2019), we assume that 15 % of biogenic monoterpene emissions form secondary organic aerosols (SOA) directly at the surface. We acknowledge that, in reality, SOA also form above the surface.

18) In section 3.1, we added a sentence to the second paragraph.

... dry radii ... While the dry radii of the dust and sea salt modes were adjusted only marginally, the dry radii of the two carbonaceous and sulfuric modes were increased significantly since their initial lifetimes were too long.

19) In section 4, we revised a sentence in the first paragraph.

... the emission of dust aerosols by cold pool outflows in the Sahara or the interaction of sea salt aerosols and shallow convective storms around the doldrums.

20) In section 4.1, we revised the first paragraph.

... Table 4 shows the aerosol burdens and fluxes of our simulation and of the CLIM simulation with ECHAM6.3-HAM2.3 averaged over the years 2003 to 2012 (Tegen et al., 2019). Table 5 shows the aerosol burdens, emissions, lifetimes, and optical depths at 550 nm of our simulation and of the AeroCom phase 3 model intercomparison, including ECHAM6.3-HAM2.3, averaged over the year 2010 (Gliß et al., 2021). ECHAM6.3-HAM2.3 used different sea salt emission schemes in the two studies leading to differences in the sea salt emissions and burdens. The values of AeroCom, comparing more than 10 models, are subject to large uncertainties. For example, the standard deviations of the lifetimes range between 29 % for organic aerosol to 91 % for sea salt. ... ECHAM6.3-HAM2.3 and AeroCom. The largest differences are observed for carbonaceous aerosols, which is caused by too low biomass burning emissions (Tegen et al., 2019; Salzmann et al., 2022). In future simulations, we plan to use wildfire emissions from the GFAS database (Kaiser et al., 2012) and anthropogenic emissions from the CEDS database (Hoesly et al., 2018; Feng et al., 2020), which are based on more recent observations and provided at higher resolutions than the AeroCom-II ACCMIP database (Heil et al., 2022).

21) In section 4.1, we revised table 4.

Global mean aerosol burdens and fluxes of ICON-HAM-lite averaged over February 2020 to January 2021 and of ECHAM6.3–HAM2.3 (CLIM simulation) averaged over the years 2003 to 2012 (Tegen et al., 2019).

	Burden (Tg)	Emission (Tg yr^{-1})	Dry depos. (Tg yr^{-1})	Wet depos. (Tg yr^{-1})
ICON-HAM-lite				
Dust	19.65	1873	1066	807.1
Sea salt	8.771	2823	369.3	2447
Carbonaceous	0.747	48.05	11.30	36.38
Sulfuric	2.817	219.2	42.90	175.5
ECHAM-HAM				
Dust	16.5	1124	447	687
Sea salt	3.9	1212	353	863
Black carbon	0.14	8.1	0.73	7.4
Organic aerosol	1.0	69.0	5.58	64.4
Sulfate	2.22	218.7	8.33	209.4

22) In section 4.1, we revised table 5.

Global mean aerosol burdens, emissions, lifetimes, and optical depths at 550 nm of ICON-HAM-lite averaged over February 2020 to January 2021 and of ECHAM6.3–HAM2.3 and AeroCom phase 3 averaged over the year 2010 (Gliß et al., 2021).

	Burden (Tg)	Emission (Tg yr^{-1})	Lifetime (d)	Optical depth
ICON-HAM-lite				
Dust	19.65	1873	3.828	0.0098
Sea salt	8.771	2823	1.133	0.0397
Carbonaceous	0.747	48.05	5.670	0.0074
Sulfuric	2.817	219.2	4.689	0.0347
ECHAM-HAM				
Dust	19.5	1170	6.0	0.031
Sea salt	10.3	5920	0.63	0.058
Black carbon	0.174	9.8	6.4	0.002
Organic aerosol	1.14	69.2	6.0	0.013
Sulfate	2.58	218.0	4.3	0.045
AeroCom phase 3 (median)				
Dust	16.6	1440	3.7	0.021
Sea salt	8.7	4980	0.56	0.044
Black carbon	0.131	9.7	5.5	0.002
Organic aerosol	1.91	116.0	6.0	0.022
Sulfate	1.80	143.0	4.9	0.035

23) In section 4.1, we revised figure 5.
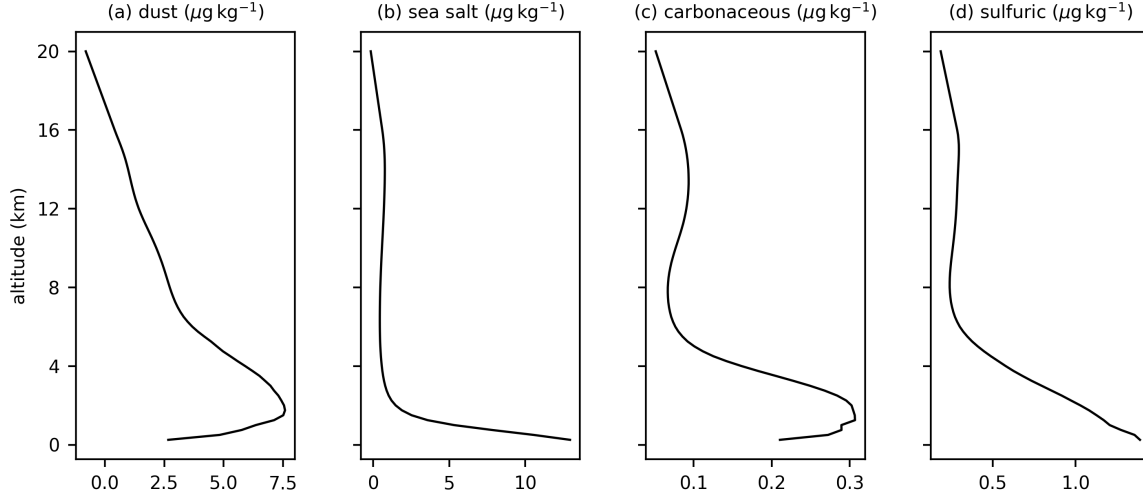
Global mean mass mixing ratios of aerosols averaged over February 2020 to January 2021: dust (a), sea salt (b), carbonaceous aerosol (c), and sulfuric aerosol (d).

24) In section 4.1, we revised three sentences in the third paragraph.

Dust aerosols are lifted up to about 6 km by convective storms, and some aerosols rise even further up to about 12 km. In contrast, sea salt aerosols are washed out by low marine clouds, and only few aerosols rise above 2 km. The profile of carbonaceous aerosols shows a local peak at about 14 km, whereas the profile of sulfuric aerosols decreases monotonically with the altitude.

25) In section 4.1, we revised a sentence in the third paragraph.

... dry radius ...

26) In section 4.1, we revised a sentence in the last paragraph.

... the optical depth of our simulation and the MODIS-Aqua satellite, i.e., the combined dark target and deep blue product (Platnick et al., 2015).

27) In section 4.1, we added a sentence to the last paragraph.

Note that observations from satellites are subject to some uncertainties as discussed by Vogel et al. (2022). On average, the optical depth of MODIS is larger than those of other satellites especially over the ocean (Vogel et al., 2022, tables 2 and 3).

28) In section 4.1, we revised figure 6.
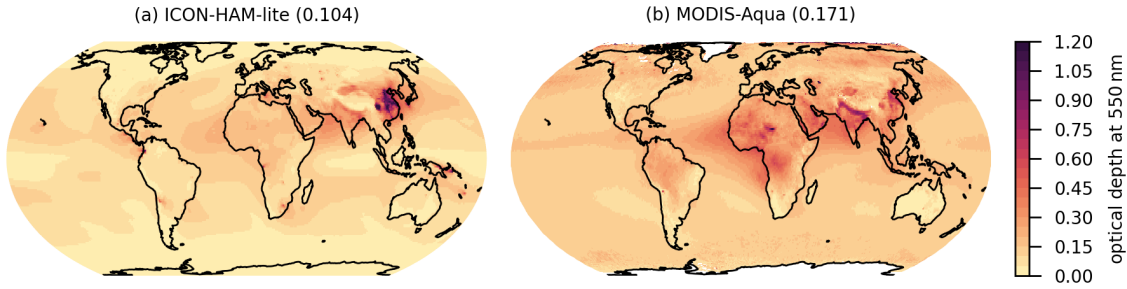
Aerosol optical depth at 550 nm of ICON-HAM-lite averaged over February 2020 to January 2021 (a) and of MODIS-Aqua, i.e., the combined dark target and deep blue product (Platnick et al., 2015), averaged over 2018 to 2022 (b). The spatial average over 60° S to 60° N is given in brackets.

29) In section 4.1, we revised a sentence in the last paragraph.

... (0.171).

30) In section 4.1, we added two sentences to the last paragraph.

The optical depths of these two modes are also lower than those of the MACv2 aerosol climatology of Kinne (2019), which is commonly used in simulations with ICON-MPIM (Hohenegger et al., 2023). The predefined optical depths are 0.031 for dust, 0.028 for sea salt, 0.022 for organic aerosol, and 0.037 for sulfate (Kinne, 2019, table 1). There are several ways to address these biases.

31) In section 4.1, we added a sentences to the last paragraph.

Third, we plan to include secondary aerosols from nucleation (Stier et al., 2005).

32) In section 4.2, we corrected a sentence in the first paragraph.

Carbonaceous aerosols are emitted by wildfires, predominantly in Central Africa and South America, and transported over the ocean by trade winds.

33) In section 4.2, we corrected a sentence in the second paragraph.

Previous studies have shown that aerosol-cloud interactions play an important role in cyclones.

34) In section 4.2, we corrected a sentence in the third paragraph.

... diverging cold pools that originate from convective downdrafts and mesoscale circulation that

lifts air at the gust front.

35) In section 4.2, we corrected a sentence in the third paragraph.

... mesoscale dynamics and the associated dust storms and need to compensate for that with the aid of tuning parameters (Marsham et al., 2011; Prein, 2023).

36) In section 5, we revised a sentence in the first paragraph.

... dry radius ...

37) In section 5, we revised a sentence in the second paragraph.

... emitted by trade winds and washed out by low marine clouds.

38) In section 5, we revised a sentence in the second paragraph.

... emitted from wildfires and transported over the ocean.

39) In section 5, we added two sentence to the last paragraph.

We plan to evaluate the aerosol processes more in-depth, to update the emission database, to fine tune parameters like aerosol size, and to add secondary aerosols from nucleation. In particular, we aim to improve the representation of the aerosol optical depth and absorption optical depth, which will be important for studies on aerosol forcing.

40) We revised the code and data availability statement.

The source code that we used to perform the simulation is available on Zenodo (Weiss et al., 2024a). The data and scripts that we used to generate the figures are available on Zenodo as well (Weiss et al., 2024b).

41) We extended the acknowledgements.

ICON-HAM-lite has been developed at the University of Oxford as a reduced complexity version of the ICON-HAM model. ICON-HAM is developed by a consortium composed of the Center for Climate Systems Modeling (ETH Zurich and MeteoSwiss), Max-Planck-Institute for Meteorology, Forschungszentrum Jülich, University of Oxford, Finnish Meteorological Institute, and Leibniz Institute for Tropospheric Research (TROPOS), and managed by TROPOS.

References

Bohren, C. F. and Huffman, D. R.: Absorption and Scattering of Light by Small Particles, John Wiley & Sons, Ltd, ISBN 9783527618156, https://doi.org/10.1002/9783527618156, 1998.

Feng, L., Smith, S. J., Braun, C., Crippa, M., Gidden, M. J., Hoesly, R., Klimont, Z., van Marle, M., van den Berg, M., and van der Werf, G. R.: The generation of gridded emissions data for CMIP6, Geoscientific Model Development, 13, 461–482, https://doi.org/10.5194/gmd-13-461-2020, 2020.

Forschungszentrum Jülich: JUPITER Exascale Development Instrument, https://www.fz-juelich.de/en/ias/jsc/systems/supercomputers/jedi, 2025.

Gliß, J., Mortier, A., Schulz, M., Andrews, E., Balkanski, Y., Bauer, S. E., Benedictow, A. M. K., Bian, H., Checa-Garcia, R., Chin, M., Ginoux, P., Griesfeller, J. J., Heckel, A., Kipling, Z., Kirkevåg, A., Kokkola, H., Laj, P., Le Sager, P., Lund, M. T., Lund Myhre, C., Matsui, H., Myhre, G., Neubauer, D., van Noije, T., North, P., Olivié, D. J. L., Rémy, S., Sogacheva, L., Takemura, T., Tsigaridis, K., and Tsyro, S. G.: AeroCom phase III multi-model evaluation of the aerosol life cycle and optical properties using ground- and space-based remote sensing as well as surface in situ observations, Atmospheric Chemistry and Physics, 21, 87–128, https://doi.org/10.5194/acp-21-87-2021, 2021.

Guenther, A., Hewitt, C. N., Erickson, D., Fall, R., Geron, C., Graedel, T., Harley, P., Klinger, L., Lerdau, M., Mckay, W. A., Pierce, T., Scholes, B., Steinbrecher, R., Tallamraju, R., Taylor, J., and Zimmerman, P.: A global model of natural volatile organic compound emissions, Journal of Geophysical Research: Atmospheres, 100, 8873–8892, https://doi.org/https://doi.org/10.1029/94JD02950, 1995.

Heil, A., Schultz, M., and Granier, C.: AeroCom II emission data, https://aerocom-classic.met.no/DATA/download/emissions/AEROCOM-II-ACCMIP/, 2022.

Hoesly, R. M., Smith, S. J., Feng, L., Klimont, Z., Janssens-Maenhout, G., Pitkanen, T., Seibert, J. J., Vu, L., Andres, R. J., Bolt, R. M., Bond, T. C., Dawidowski, L., Kholod, N., Kurokawa, J.-I., Li, M., Liu, L., Lu, Z., Moura, M. C. P., O'Rourke, P. R., and Zhang, Q.: Historical (1750–2014) anthropogenic emissions of reactive gases and aerosols from the Community Emissions Data System (CEDS), Geoscientific Model Development, 11, 369–408, https://doi.org/10.5194/gmd-11-369-2018, 2018.

Hohenegger, C., Kornblueh, L., Klocke, D., Becker, T., Cioni, G., Engels, J. F., Schulzweida, U., and Stevens, B.: Climate Statistics in Global Simulations of the Atmosphere, from 80 to 2.5 km Grid Spacing, Journal of the Meteorological Society of Japan. Ser. II, 98, 73 – 91, https://doi.org/10.2151/jmsj.2020-005, 2020.

Hohenegger, C., Korn, P., Linardakis, L., Redler, R., Schnur, R., Adamidis, P., Bao, J., Bastin, S., Behravesh, M., Bergemann, M., Biercamp, J., Bockelmann, H., Brokopf, R., Brüggemann, N., Casaroli, L., Chegini, F., Datseris, G., Esch, M., George, G., Giorgetta, M., Gutjahr, O., Haak, H., Hanke, M., Ilyina, T., Jahns, T., Jungclaus, J., Kern, M., Klocke, D., Kluft, L., Kölling, T., Kornblueh, L., Kosukhin, S., Kroll, C., Lee, J., Mauritsen, T., Mehlmann, C., Mieslinger, T., Naumann, A. K., Paccini, L., Peinado, A., Praturi, D. S., Putrasahan, D., Rast, S., Riddick, T., Roeber, N., Schmidt, H., Schulzweida, U., Schütte, F., Segura, H., Shevchenko, R., Singh, V., Specht, M., Stephan, C. C., von Storch, J.-S., Vogel, R., Wengel, C., Winkler, M., Ziemen, F., Marotzke, J., and Stevens, B.: ICON-Sapphire: simulating the components of the Earth system and their interactions at kilometer and subkilometer scales, Geoscientific Model Development, 16, 779–811, https://doi.org/10.5194/gmd-16-779-2023, 2023.

Kaiser, J. W., Heil, A., Andreae, M. O., Benedetti, A., Chubarova, N., Jones, L., Morcrette, J.-J., Razinger, M., Schultz, M. G., Suttie, M., and van der Werf, G. R.: Biomass burning emissions estimated with a global fire assimilation system based on observed fire radiative power, Biogeosciences, 9, 527–554, https://doi.org/10.5194/bg-9-527-2012, 2012.

Kinne, S.: The MACv2 aerosol climatology, Tellus B: Chemical and Physical Meteorology, 71, 1–21, https://doi.org/10.1080/16000889.2019.1623639, 2019.

Marsham, J. H., Knippertz, P., Dixon, N. S., Parker, D. J., and Lister, G. M. S.: The importance of the representation of deep convection for modeled dust-generating winds over West Africa during summer, Geophysical Research Letters, 38, https://doi.org/10.1029/2011GL048368, 2011.

Platnick, S., Hubanks, P., Meyer, K., and King, M. D.: MODIS Atmosphere L3 Monthly Product (08_L3), `https://modis.gsfc.nasa.gov/data/dataprod/mod08.php`, 2015.

Pöhlker, M. L., Pöhlker, C., Quaas, J., Mülmenstädt, J., Pozzer, A., Andreae, M. O., Artaxo, P., Block, K., Coe, H., Ervens, B., Gallimore, P., Gaston, C. J., Gunthe, S. S., Henning, S., Herrmann, H., Krüger, O. O., McFiggans, G., Poulain, L., Raj, S. S., Reyes-Villegas, E., Royer, H. M., Walter, D., Wang, Y., and Pöschl, U.: Global organic and inorganic aerosol hygroscopicity and its effect on radiative forcing, Nature Communications, 14, 6139, https://doi.org/10.1038/s41467-023-41695-8, 2023.

Prein, A. F.: Thunderstorm straight line winds intensify with climate change, Nature Climate Change, 13, 1353–1359, https://doi.org/10.1038/s41558-023-01852-9, 2023.

Salzmann, M., Ferrachat, S., Tully, C., Münch, S., Watson-Parris, D., Neubauer, D., Siegenthaler-Le Drian, C., Rast, S., Heinold, B., Crueger, T., Brokopf, R., Mülmenstädt, J., Quaas, J., Wan, H., Zhang, K., Lohmann, U., Stier, P., and Tegen, I.: The Global Atmosphere-aerosol Model ICON-A-HAM2.3–Initial Model Evaluation and Effects of Radiation Balance Tuning on Aerosol Optical Thickness, Journal of Advances in Modeling Earth Systems, 14, e2021MS002 699, https://doi.org/10.1029/2021MS002699, 2022.

Seifert, A. and Beheng, K. D.: A two-moment cloud microphysics parameterization for mixed-phase clouds. Part 1: Model description, Meteorology and Atmospheric Physics, 92, 45–66, https://doi.org/10.1007/s00703-005-0112-4, 2006.

Siebesma, A. P., Bony, S., Jakob, C., and Stevens, B., eds.: Clouds and Climate: Climate Science's Greatest Challenge, Cambridge University Press, Cambridge, https://doi.org/10.1017/9781107447738, 2020.

Stier, P., Feichter, J., Kinne, S., Kloster, S., Vignati, E., Wilson, J., Ganzeveld, L., Tegen, I., Werner, M., Balkanski, Y., Schulz, M., Boucher, O., Minikin, A., and Petzold, A.: The aerosol-climate model ECHAM5-HAM, Atmospheric Chemistry and Physics, 5, 1125–1156, https://doi.org/10.5194/acp-5-1125-2005, 2005.

Tegen, I., Harrison, S. P., Kohfeld, K., Prentice, I. C., Coe, M., and Heimann, M.: Impact of vegetation and preferential source areas on global dust aerosol: Results from a model study, Journal of Geophysical Research: Atmospheres, 107, AAC 14–1–AAC 14–27, https://doi.org/https://doi.org/10.1029/2001JD000963, 2002.

Tegen, I., Neubauer, D., Ferrachat, S., Siegenthaler-Le Drian, C., Bey, I., Schutgens, N., Stier, P., Watson-Parris, D., Stanelle, T., Schmidt, H., Rast, S., Kokkola, H., Schultz, M., Schroeder, S., Daskalakis, N., Barthel, S., Heinold, B., and Lohmann, U.: The global aerosol–climate model ECHAM6.3–HAM2.3 – Part 1: Aerosol evaluation, Geoscientific Model Development, 12, 1643–1677, https://doi.org/10.5194/gmd-12-1643-2019, 2019.

Vogel, A., Alessa, G., Scheele, R., Weber, L., Dubovik, O., North, P., and Fiedler, S.: Uncertainty in Aerosol Optical Depth From Modern Aerosol-Climate Models, Reanalyses, and Satellite Products, Journal of Geophysical Research: Atmospheres, 127, e2021JD035 483, https://doi.org/10.1029/2021JD035483, e2021JD035483 2021JD035483, 2022.

Weiss, P., Herbert, R., and Stier, P.: Code for "ICON-HAM-lite: simulating the Earth system with interactive aerosols at kilometer scales", https://doi.org/10.5281/zenodo.14335069, 2024a.

Weiss, P., Herbert, R., and Stier, P.: Data for "ICON-HAM-lite: simulating the Earth system with interactive aerosols at kilometer scales", https://doi.org/10.5281/zenodo.14393773, 2024b.